Modelling the Tunnelling Probability of an Electron Passing Through a Schottky Barrier

Author:
Daniel MEILAK

Supervisors:
Dr. Matt PROBERT
Dr. Phil HASNIP

Thesis submitted in fulfillment of the requirements for the degree of Master of Physics

UNIVERSITY OF YORK
Department of Physics

May 3, 2016

THE UNIVERSITY of York

UNIVERSITY OF YORK

Abstract

Department of Physics

Master of Physics

Modelling the Tunnelling Probability of an Electron Passing Through a Schottky Barrier

by Daniel MEILAK

This study focuses on understanding the tunnelling probability of electrons through a Schottky barrier, a potential barrier with rectifying behaviour, formed in a metal-semiconductor junction. Schottky barriers show promise in being able to allow the transmission of spin polarised electron currents into semiconductors, due to which they have seen recent interest in spintronics.

We shall attempt to study Schottky barriers by using the time independent Schrödinger equation for a single electron passing through a potential barrier. Since this is a second order ordinary differential equation, we can solve it numerically by using a differential equation solver, such as the 4th order Runge-Kutta method, to find the values of the wavefunction at each point in space.

By using a potential barrier of the form of a Schottky barrier, we are able to find the transmission probability of an electron tunnelling through the Schottky barrier for different values of temperature, or electron energy. In addition to this, by changing the height and width of the barrier, as well as using an applied bias over it, we gain an appreciation for the effect of these parameters on the transmission of the electron through the barrier.

Contents

List of Figures

List of Abbreviations

ODE	**O**rdinary **D**ifferential **E**quation
RK	**R**unge **K**utta
RKF	**R**unge **K**utta **F**ehlberg
SB	**S**chottky **B**arrier
TISE	**T**ime **I**ndependant **S**chrödinger **E**quation
WKB	**W**entzel **K**ramers **B**rillouin

Physical Constants

Reduced Planck constant	$\hbar = 1.054\,571\,80 \times 10^{-34}\,\mathrm{J\,s}$
Mass of electron	$m = 9.109\,383\,56 \times 10^{-31}\,\mathrm{kg}$
Boltzmann constant	$k_B = 1.380\,648\,53 \times 10^{-23}\,\mathrm{J\,K^{-1}}$

List of Symbols

ξ	Electric field in a Schottky barrier
E	Energy
E_{00}	Property of bulk semiconductor
E_F^m	Metal Fermi level
E_F^s	Semiconductor Fermi level
ΔE	Difference in electron energy and barrier height
I	Current
k	Wavenumber
R	Reflection coefficient
t	Time
T	Transmission coefficient
V	Voltage
$V(x)$	Potential barrier height
V_d	Diffusion potential
x	Distance
Φ_b	Barrier height
Φ_m	Metal workfunction
Φ_s	Semiconductor workfunction
Ψ	Wavefunction
Ψ_{in}	Incident wavefunction
Ψ_r	Reflected wavefunction
Ψ_t	Transmitted wavefunction
χ_s	Electron affinity

Chapter 1

Introduction

In a world dominated by technology, understanding of the core principles of electron movement through metals and semiconductors has been the linchpin on which the tech industry has advanced. The behaviour of materials such as silicon has been put into use long before those properties were understood, however, it was only after quantum mechanics had become well established, that large strides of improvement were made.

Nowadays, the latest advances of technology are very quickly incorporated into the newest consumer technologies, a huge industry that creates incentive for new studies and rapid advancement. However this does not mean that every aspect of technology is at the forefront of research. Indeed there are still many materials that rely on old, incomplete theories, that don't fully explain the materials properties. One such example, which shall be the focal point of this thesis, is the metal-semiconductor junction; and more precisely one that forms a Schottky Barrier.

1.1 Schottky Barriers and Spintronics

Schottky Barriers, named after Walter H. Schottky, form naturally between most metal-semiconductor junctions. They are potential barriers that affect the movement of electrons from one side of the interface to the other. In particular, they exhibit a rectifying behaviour, meaning that they are able to stop electrons passing through either side of the interface and only allow them to move in one direction; from the metal to the semiconductor. Through engineering the shape of a Schottky barrier, we can cause it to have properties of spin injection and accumulation, so that we have an even finer control over the electrons able to traverse it[1].

Schottky Barriers have seen recent interest in the field of spintronics (spin transport electronics) where materials are made to take advantage of not only the charge of electrons, but also their spin[2, 3]. The first electronic device to incorporate the spin of the electron was the spin valve, developed in the late 1980s. This device exhibited a magnetoresistance effect due to the spin dependant transport

of current into its ferromagnetic layers. By combining the device with semiconductors, it is expected that it could lead to new materials with fast, non-volatile memory and energy efficient processing power.

One of the main problems with this, however, is that polarised spin injection has been a very difficult property to come by[4, 5]. It is observed in magnetic semiconductors only at low temperatures, which negates their usefulness. Ferromagnetic metals can also generate spin polarized currents as they will contain excess carriers aligned to the direction of magnetisation of the material. However passing this current into a semiconductor is hard as the resistance of the metal is much lower, a problem known as the conductivity mismatch. As the semiconductor is non-magnetic, the accumulation of current passing into it will not be spin polarized.

A potential barrier, such as a Schottky barrier, will solve this problem as its rectifying behaviour will only allow spin polarised electrons to pass into the semiconductor and accumulate there. To fulfil such requirements efficiently, the SB must be constructed correctly and the materials used to form the SB must have been combined abruptly so that there is no intermixing.

1.2 A Theoretical Approach

To study the SB we shall be using a quantum mechanical approach. The Schrödinger equation can completely describe the quantum state of a system, hence we shall be using it to describe the SB by looking at the transmission probability of a single electron passing through a potential barrier. This can then be expanded to a current of electrons, which will exhibit similar properties.

Since the potential is time-independent, we shall be using the time independent Schrödinger equation (TISE), and we shall assume that, parallel to the interface, the shape of the barrier is uniform and the kinetic energy of electrons is negligible, hence we can represent it in 1D. The equation we shall study is as follows:

$$-\frac{\hbar^2}{2m}\frac{\mathrm{d}^2\Psi}{\mathrm{dx}^2} + V\Psi = E\Psi \tag{1.1}$$

The wavefunction Ψ will determine the properties of an electron, which has energy, E, and is affected by the potential barrier of height V. We can also simplify equation 1.1 by using atomic units.

$$-\frac{1}{2}\frac{\mathrm{d}^2\Psi}{\mathrm{dx}^2} + V\Psi = E\Psi \tag{1.2}$$

Hence, we need to solve a second order ordinary differential equation of one variable (x). Were the potential to be zero across all space, this equation could be trivially solved and would reveal a harmonic motion. However to solve this equation for a non-zero potential, and one that will vary with space, $V(x)$, we require a computational ODE solving method. This shall be the main method through which results shall be obtained for this paper.

1.3 Chapter Summary

This thesis is divided into five further chapters. Chapter 2 shall cover the history of study of Schottky barriers, their formation and quantum mechanical tunnelling through them. Chapter 3 will go through the various techniques used to solve the Schrödinger Equation, assessing the pros of some popular methods over others. The requirements of the program used to solve the TISE, as well as its expected output shall also be explained. Chapter 4 will be an assessment of the methods used. In it we shall go over several tests that check the validity of early results, to make sure that any later results are correct and reliable. Chapter 5 shall be used to show the various results gained over the course of this work, and shall also have some reflection on the meaning of those results in comparison to what was expected. Finally, chapter 6 shall be a conclusion for this work and give some suggestions for further work on this topic.

Chapter 2

Theory of Schottky Barriers

2.1 Historical

The first observation of the asymmetrical electrical conduction between a metal and semiconductor was by Braun who saw it in copper contacted with iron sulphide around 1874[6]. The rectification mechanism in these contacts was not fully understood, however they were used extensively as detectors in early experiments on radio. The rise of broadcasting in the 1920s was aided by the 'cat's-whisker' rectifier, a tungsten point in contact with lead sulphide which exhibited the same observed properties.

It was Schottky, Störmer and Waibel (1931) who took the first steps towards understanding the phenomena. They saw that when current flowed through the interface, a potential drop occurs almost entirely at the contact which hinted at the existence of a potential barrier. At first it was thought that quantum mechanical tunnelling was the cause of the rectifying behaviour, however it was found that this would result in a net current flow opposite to that observed. In 1938 Schottky and Mott independently showed that the process of drift and diffusion could properly explain the direction of rectification[6].

The next breakthrough in understanding what would later come to be known as the Schottky Barrier would be by Bethe, who would develop thermionic-emission theory explaining the emission of electrons into a metal. Interest in SBs would continue to be driven by advances in semiconductor technology and the need for smaller and faster devices.

2.2 Formation

The formation of a Schottky Barrier between a metal and semiconductor is dependant on many factors. These range from the doping level of the semiconductor to the workfunction of the metal (Φ_m) and of the semiconductor (Φ_s), which (for a metal) is the minimum amount of energy required to excite an electron from the Fermi level to the vacuum level outside the surface of the metal. The way contact

occurs, whether it is abrupt or happens gradually, can affect the resulting potential barrier. If not done correctly, an Ohmic contact can form, where there is no rectifying behaviour and current can pass according to a linear I-V curve, as with Ohms Law.

The majority of contacts are formed by an n-type semiconductor, i.e. one where electrons are the majority charge carrier and holes are a minority, with a workfunction less than that of the metal. While isolated, as shown in figure 2.1(a), the two materials can be connected electrically by an ideal wire, allowing electrons in the conduction band of the semiconductor to flow into the metal, causing the Fermi levels to equalize (figure 2.1(b)). This creates a depletion region in the semiconductor where positive donor ions remain fixed in place, which in turn causes a potential gradient, giving rise to the Schottky Barrier of height Φ_b. Due to the difference in charge over the barrier, from the excess electrons in the metal and the uncompensated positive ions in the semiconductor, an electric field is also in effect over the whole of the depletion region.

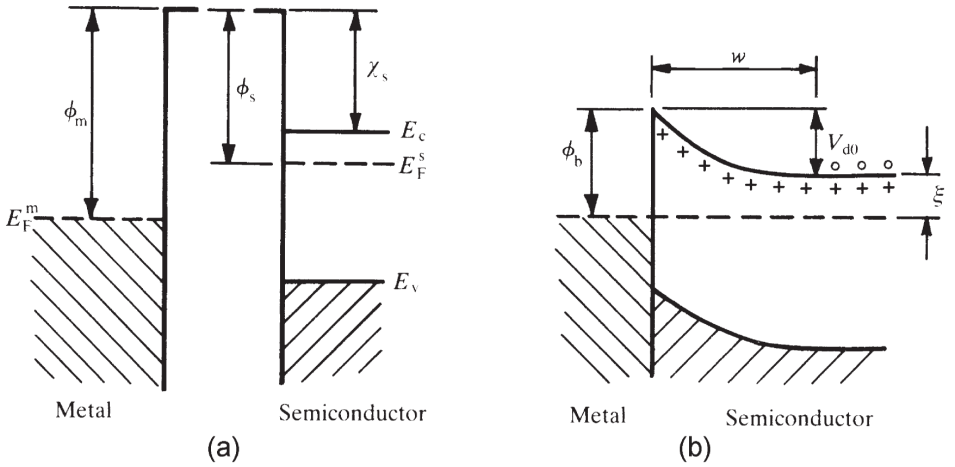

FIGURE 2.1: Band diagrams showing the formation of a Schottky Barrier between a metal and an n-type semiconductor a)neutral and isolated; b) electrically connected in perfect contact. Figure adapted from Rhoderick.[6]

It should be noted that normally, as the two sides are brought into contact with each other, they will remain separated by a layer of oxide from the side of the semiconductor, however the electrons will be able to tunnel through this and, to an approximation, its effects are negligible. Indeed we shall assume the ideal case where no such insulating layer exists. Schottky and Mott theorised that the height of the barrier could be given by

$$\Phi_b = \Phi_m - \chi_s \tag{2.1}$$

This equation is the Schottky-Mott limit, which shows that the height of the Schottky Barrier is a function of the workfunction of the metal and the electron affinity, χ_s, of the semiconductor. The electron affinity of a semiconductor is taken as the energy difference between the bottom of the conduction band to the vacuum level outside the surface. Again, we must note that equation 2.1 is a first order approximation to the height of the barrier and in most cases experimental data will not agree with this. This limit assumes that the aforementioned oxide layer doesn't exist, that the surface dipole contributions to Φ_m and χ_s do not change when the metal and semiconductor come into contact and, most importantly, that the contact between the two materials is abrupt with no defects or intermixing of materials.

2.3 Transport Mechanisms

Once a Schottky barrier is formed, there a several mechanisms for electrons to move between the metal and semiconductor. Figure 2.2 shows the four main mechanisms for an electron to overcome the SB in an n-doped semiconductor in forward bias. These are:

1. emission of electrons over the barrier
2. quantum mechanical tunnelling through the barrier
3. recombination in the space charge region
4. recombination in the neutral region

Mechanism (1) occurs for electrons which have an energy higher than the top of the barrier and is the main method through which electrons move across the barrier. We usually consider an ideal Schottky barrier to be one where this is the only mechanism taking place. However we will be focusing on the quantum mechanical tunnelling which deviates from the ideal behaviour.

It is known that in the quantum mechanical world there is a non-zero probability of electrons with an energy lower than the full barrier height to pass through it, and similarly a less that 100% chance that electrons with an energy higher to do the same. For Schottky Barriers, tunnelling is more likely in heavily doped semiconductors as the depletion region is shorter due to the more densely packed donors.

The quantum mechanical tunnelling can be further split into two regimes. At low temperatures, where electrons have energies close to that of the Fermi Level, tunnelling from the bottom of the semiconductor conduction band is known as Field Emission. At higher

temperatures, where electrons are excited and tunnelling probability increases due to a lower perceived barrier and narrower barrier width, this becomes Thermionic Field Emission. However, as the electrons energies follow a Fermi-Dirac distribution, the percentage of electrons that follow the TFE regime is far lower than that of FE[6]. This is because the majority of electrons will be at a temperature (and therefore energy) far lower than the height of the barrier while there will be a small quantity of excited electrons with energy close to the top. Finally, at an energy higher than that of the barrier height, electrons follow mechanism (1) as shown in figure 2.2. We must remember that even during emission over the barrier, particularly at energies just over it, there will be a non-zero probability of electrons being reflected away from the barrier.

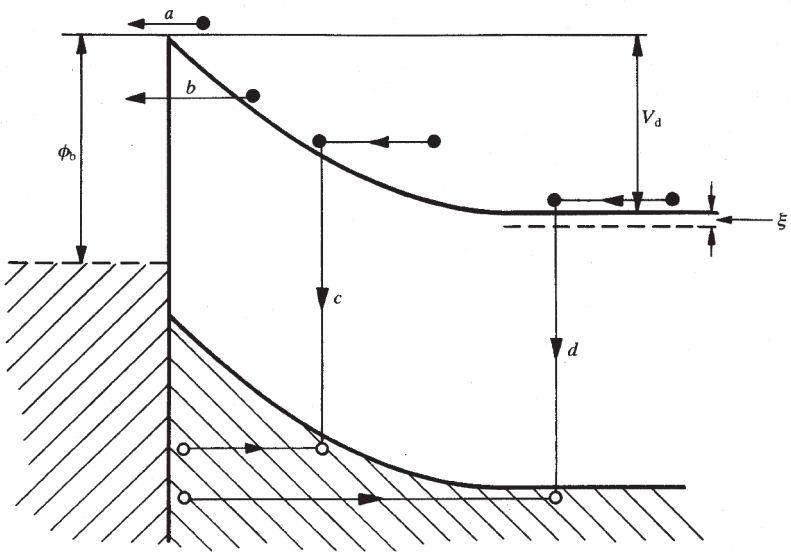

FIGURE 2.2: Transport mechanisms across a Schottky Barrier on n-type semiconductor in forward bias, a) emission over the barrier, b) tunnelling through the barrier, c) recombination in the space charge region, d) recombination in the neutral region.

Chapter 3

Computational Approach

3.1 Choosing an ODE solver

As stated in the introduction, the aim of this project is to use the time independent Schrödinger Equation for an electron passing through the Schottky Barrier. We shall attempt to solve the TISE using a numerical ordinary differential equation solver suitable for this specific task. Hence, we first need to understand the requirements of our ODE solver, whether it be oriented towards finding a solution quickly, or very reliable in the case of discontinuities. Similarly, the output of our program must be suitable for analysis and produce well defined results.

3.1.1 The Runge-Kutta Method

The Runge-Kutta methods of different orders are very commonly used for solving differential equations. They arise from a modification to the Euler Method, one of the simplest possible ODE solvers, but have many benefits over it. One of the main advantages of the methods is that it does not require the calculation of derivatives of the function as we use the Taylor approximation for them. Any Runge-Kutta method can be represented by a Butcher tableau[7] which contains the coefficients used in the RK algorithm. We shall be using the 4th order RK method as this is commonly seen as the most efficient. This is because it has a high enough order truncation error to give us good approximations while also not being too computationally expensive in terms of function evaluations. Figure 3.1 shows the Butcher tableau for this method.

$$
\begin{array}{c|cccc}
0 & & & & \\
\frac{1}{2} & \frac{1}{2} & & & \\
\frac{1}{2} & 0 & \frac{1}{2} & & \\
1 & 0 & 0 & 1 & \\
\hline
 & \frac{1}{6} & \frac{2}{6} & \frac{2}{6} & \frac{1}{6}
\end{array}
$$

FIGURE 3.1: Butcher Tableau for the 4th order Runge-Kutta method.

From the algorithm, we can see that the method splits the real axis into steps of size h and calculates an approximation to each step using four intermediate values $k1, k2, k3, k4$, which rely on previous steps and function evaluations. In fact, at each step, to produce an answer of fourth order accuracy, it requires four function evaluations. In practice this method is very robust; it handles discontinuities well and, as we have seen from the theorised shape of SBs, discontinuities are to be expected. We also know that the method handles larger step sizes well and therefore should be efficient, however it is a general ODE solving method and is not specialised at solving ODE's of the form of the TISE[7].

3.1.2 The Numerov Method

As was hinted in the last section, The Numerov Method[8] is one such method that specialises at solving equations of the form

$$\frac{\mathrm{d}^2 y}{\mathrm{dx}^2} = f(x)y(x) \tag{3.1}$$

This includes the time independent Schrödinger equation. It is a multistep method that exploits the special structure of the equation to produce a method that has fifth order accuracy while only requiring two function evaluations per step. Like the 4th order RK method, it is derived by Taylor expanding the $y(x+h)$ and $\frac{\mathrm{d}^2 y}{\mathrm{dx}^2}$ terms. This method is therefore the preferred method for solving the Schrödinger equation however it does come with a few drawbacks. This method requires a different ODE solving method (usually of low order) to generate the first step, and also from this, is not good at handling discontinuities. Since we know we will have to deal with discontinuities in the potential barrier, it may be troublesome if we try to use this method.

3.1.3 The Runge-Kutta-Fehlberg Method

To achieve their benefits, the above methods must either sacrifice some usability or efficiency in solving the TISE. However there is one other method that we have not yet considered. The Runge-Kutta-Fehlberg method is a modification of the general RK methods which takes a 4th and 5th order RK method with similar intermediate steps and combines them to produce a 5th order method with error control. The error control is what makes this a viable alternative, since, although we will have to make two further function evaluations, the step size shall vary between each step so that there is minimal truncation error. That is, the difference between the methods approximation, and the exact solution, is kept to a minimum at each step. Figure 3.2 shows the Butcher tableau for the RKF method.

0						
$\frac{1}{4}$	$\frac{1}{4}$					
$\frac{3}{8}$	$\frac{3}{32}$	$\frac{9}{32}$				
$\frac{12}{13}$	$\frac{1932}{2197}$	$-\frac{7200}{2197}$	$\frac{7296}{2197}$			
1	$\frac{439}{216}$	-8	$\frac{3680}{513}$	$-\frac{845}{4104}$		
$\frac{1}{2}$	$-\frac{8}{27}$	2	$-\frac{3544}{2565}$	$\frac{1859}{4104}$	$-\frac{11}{40}$	
(a)	$\frac{25}{216}$	0	$\frac{1408}{2565}$	$\frac{2197}{4104}$	$-\frac{1}{5}$	
(b)	$\frac{16}{135}$	0	$\frac{6656}{12825}$	$\frac{28561}{56430}$	$-\frac{9}{50}$	$\frac{2}{55}$

FIGURE 3.2: Butcher Tableau for the Runge-Kutta-Fehlberg method.

It should be noted that in practice, while using this method, we found that although the solving of the ODE worked without trouble, the error control would always fail somewhat when reaching a discontinuity. As the algorithm would reach the discontinuity, it would move over it and find that the value of the function (the potential) at either side would be drastically different, and would redo the step with a smaller size. This would go on for lower and lower step sizes until the minimum step size tolerance was reached, and cause the program to stop with an error message. However, by adjusting the standard algorithm for this method, we found that we could get past this, albeit with slightly less reliability, by stopping it from repeatedly lowering the step size and instead sticking to a minimum until it passed the discontinuity. It is recommended that if this method is to be used, it should be backed up with some usage of the 4th order RK method to make sure that results are always consistent[7].

3.2 The Program

3.2.1 Restructuring the TISE

Due to the need for a good handling of discontinuities, we have chosen to move forward with the fourth order Runge-Kutta method and therefore we must now translate the TISE into something that can be used in the RK algorithm. The RK method solves a first order ODE, while our TISE is in fact second order (it has a second derivative term). To combat this, we can turn the TISE into a system of two first order ODE using the substitution

$$\begin{aligned} \mathbf{u'} &= \Psi'' \\ u^{(1)} &= \Psi, u^{(2)} = \Psi' \end{aligned} \tag{3.2}$$

Hence from 1.2 we have

$$\mathbf{u'} = \begin{pmatrix} u^{(2)} \\ [V(x) - E]u^{(1)} \end{pmatrix} \tag{3.3}$$

3.2.2 The Potential Barrier V(x)

From figure3.3 we can see that our system of ODEs contains a function, $V(x)$, the potential barrier, which we shall use to simulate a Schottky Barrier. This must be well defined, and its value worked out at every step of the calculation. We have also chosen that the program allows us to change the shape of this potential so that we can start from a simple barrier, which we will be able to test, to a more complex one which we can study.

The simplest barrier (barring the trivial case of a constant zero potential) that we shall study, is the rectangular barrier. This has well defined solutions that are simple to test. Attempting to move towards a structure more similar to those shown in figure 2.1 , we can also use a triangular barrier, which should show signs of a transition between tunnelling in the Field Emission regime at low temperatures (energy) and later Thermionic Field Emission at higher temperatures.

Multiple barriers should also be examinable, such as double square or triangular barrier, as well as a mixture of these to create trapezium like structures. Finally, current studies suggest that the Schottky barrier structure would be an immediate vertical barrier followed by a parabolic decline. Figure 3.3 shows a few examples of potential barriers that have been coded into the program, however with little change, many more functional forms should be possible.

3.2.3 The First Approximation

As with all solutions to an ODE, we must start with initial conditions. To make our lives simpler we have chosen to start our solving of the TISE from the exiting side of the potential barrier. Figure 3.4 illustrates how the solver shall run. We assume that the wavefunction on the right hand side is only made of one component, the wavefunction for an electron exiting the barrier, Ψ_t. This means that there will be no reflection of plane waves from further inside the semiconductor.

Inside the barrier the wavefunction is split into two components, that of an electron entering the barrier and also one that has bounced off the right hand side and is moving back to the left. Finally on the left hand side we have another split of the wavefunction for an electron heading towards the barrier, Ψ_{in} and one that has failed to enter

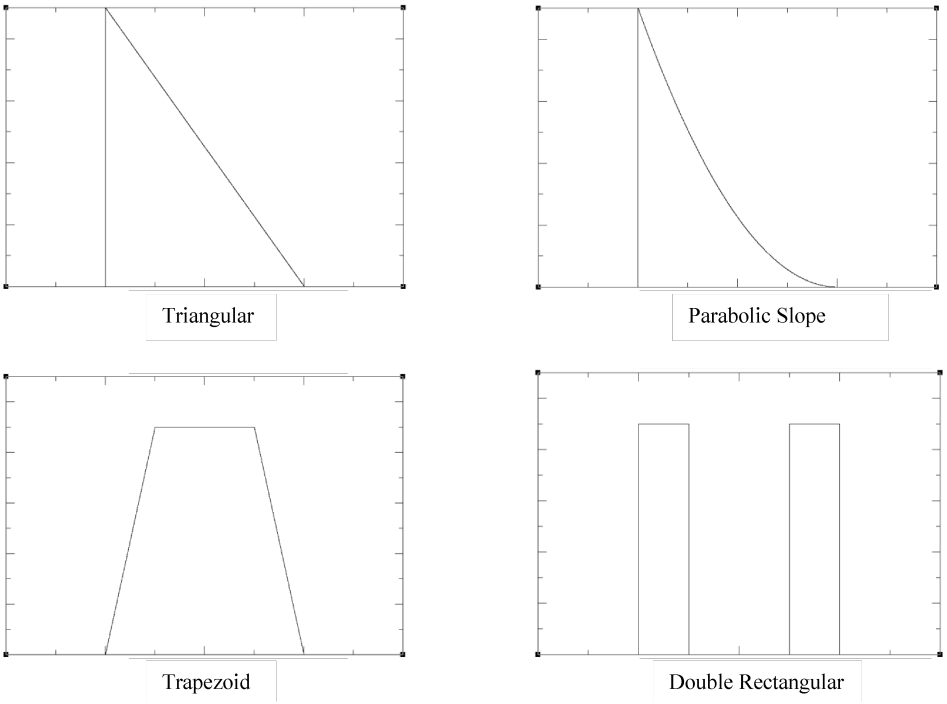

FIGURE 3.3: Various potential barrier shapes usable in the program.

it and has immediately bounced back, Ψ_r.

Our initial assumption and setup allows us to very easily work out an initial approximation for the wavefunction **u'**. From solving the Schrödinger Equation for an election outside of any potential barrier, i.e. where $V(x) = 0$, we know that the functional form of the wavefunction is a complex exponential, or plane-wave, hence

$$\begin{aligned} \Psi &= A\exp(ikx) + B\exp(-ikx) \\ \Psi' &= iAk\exp(ikx) - iBk\exp(-ikx) \end{aligned} \tag{3.4}$$

Where A and B are arbitrary complex numbers and k is the wavenumber, the frequency of oscillations in space. We know, however, that when exiting the barrier, our wavefunction will only consist of one component since there is no reflection of plane waves, so $B = 0$. We also know that the wavenumber is related to the energy of the electron (in 1D) by

$$E = \frac{\hbar^2 k^2}{2m} \tag{3.5}$$

Hence, with the chosen energy of the electron, we can work out the wavenumber k and therefore also an initial approximation for Ψ and Ψ'.

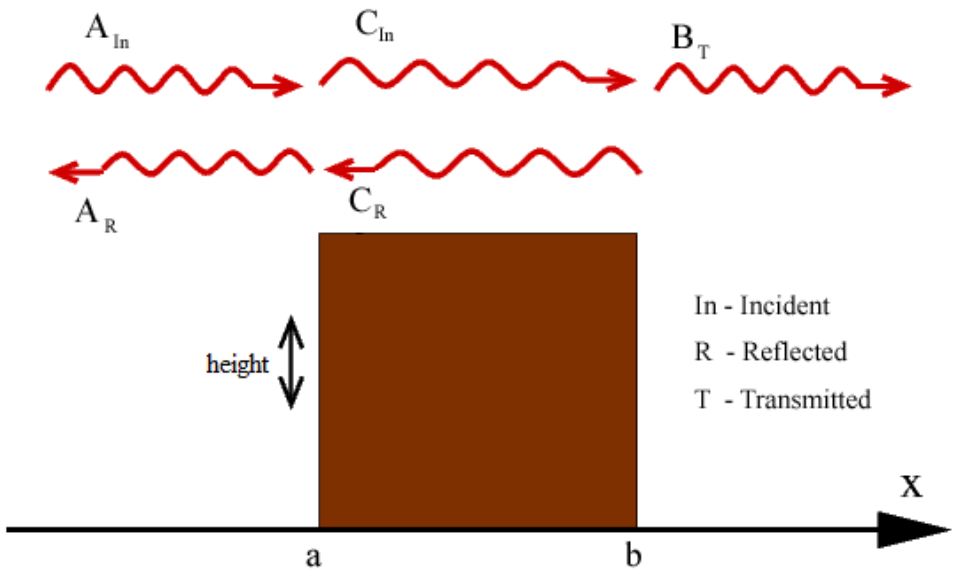

FIGURE 3.4: Simple representation of the wavefunction of the electron as it passes through the barrier.

3.2.4 Finding the Transmission Coefficient

With our well defined function, $V(x)$, and initial conditions, Ψ_0 and Ψ_0', the program should now be able to output an approximation to the TISE at each point in space. These points will give the values of the wavefunction and its derivative, however it will not immediately give the probability of transmission of an electron through the barrier. For this we require a little more work.

The probability of an electron passing through the barrier can also be represented by the transmission coefficient. Since, in our system, no electrons leaving the barrier are reflected back, this coefficient is the same as the probability of passing through the barrier. We also know that the transmission coefficient is related to the reflection coefficient

$$T = 1 - R \tag{3.6}$$

Hence by finding one of the two, we can work out the other. Let us take the full wavefunction on the left hand side of fig.

$$\begin{aligned} \Psi &= \Psi_{in} + \Psi_r \\ \Psi &= A\exp(ikx) + A_r\exp(-ikx) \end{aligned} \tag{3.7}$$

The coefficients A and A_r can be used to work out R (and T) since

$$\frac{|A_r|^2}{|A|^2} = R \tag{3.8}$$

Hence we need to solve 3.7 to find A and A_r in terms of the value of the wavefunction, which we shall have the data for. Choosing x-values of 0 and $\frac{\pi}{2k}$.

$$\begin{aligned} \Psi(0) &= A + A_r \\ \Psi(\frac{\pi}{2k}) &= i(A - A_r) \end{aligned} \tag{3.9}$$

And after rearranging

$$\begin{aligned} A &= \frac{1}{2}(\Psi(0) - \Psi(\frac{\pi}{2k})) \\ A_r &= \frac{1}{2}(\Psi(0) + \Psi(\frac{\pi}{2k})) \end{aligned} \tag{3.10}$$

Hence, by using the program's output at $x = 0$ and $x = \frac{\pi}{2k}$ we can work out A and A_r from 3.10 and also R from 3.8.

3.2.5 Plotting "I-V" Graphs

The study of potential barriers is very often done through the usage of current against voltage graphs. Applying a voltage across a potential barrier has several effects depending on the type of bias applied. In the forward bias we would have the metal (hole dominated) side of the barrier connected to a positive terminal, and the semiconductor (electron abundant) side of the barrier connected to a negative terminal. This leads to the holes in the metal being pushed towards the junction between the materials, due to the positive terminal repelling them, and similarly the electrons in the semiconductor. There will be a change in potential between both materials which will have an effect on the SB. The Fermi level of the semiconductor is lifted relative to the metal Fermi level, reducing the barrier height, and narrowing the depletion width (the width of the barrier). This combination of factors causes the current flow through the barrier to increase.

In the reverse bias the opposite happens. The semiconductor is connected to a negative terminal and the metal to a positive terminal. The holes and electrons on either side of the junction are pushed further apart. This leads to the Fermi level of the semiconductor dropping relative to that of the metal and hence the barrier height increases, while the depletion region becomes wider. Figure 3.5 shows the shape of the barrier in the two cases.

It is therefore simple to simulate an applied voltage by using a barrier with potentials at different levels on either side. Measuring the current is, unfortunately, not as obvious. This project relies on

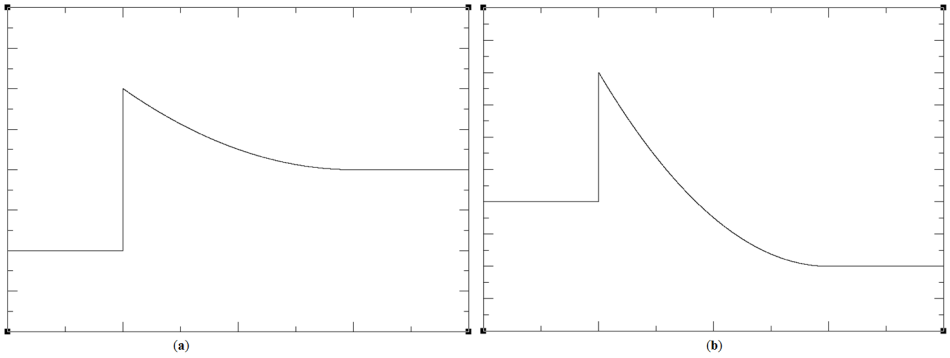

FIGURE 3.5: The Schottky Barrier under forward (a) and backward (b) bias.

finding the probability of a single electron passing through the barrier hence we will not be able to see a direct increase in current. However, by looking at the transmission coefficient, we can see the probability for the current being able to pass. Hence, we shall plot graphs of T against voltage. We will not be able to study the reverse bias regime as we assume that we do not have any electrons tunnelling back through the barrier from the semiconductor, and therefore cannot have a negative current.

3.2.6 Flow Chart and other Scripts

Figure 3.6 below shows the flow of the program, named "runge_kutta.f90" and a copy of it can be found in appendix A with appropriate commentary.

Finally, there are a few other scripts that were used to collect data from the main program. Most of these took the form of a shell script that would execute the main program for a range of parameters, including potential height, width and electron energies.One of these has also been included into the appendix (B)to give the reader an idea of the flexibility of the program as well as a head start if they wish to perform calculations with parameters outside of those studied here, or with drastically different potential barriers.

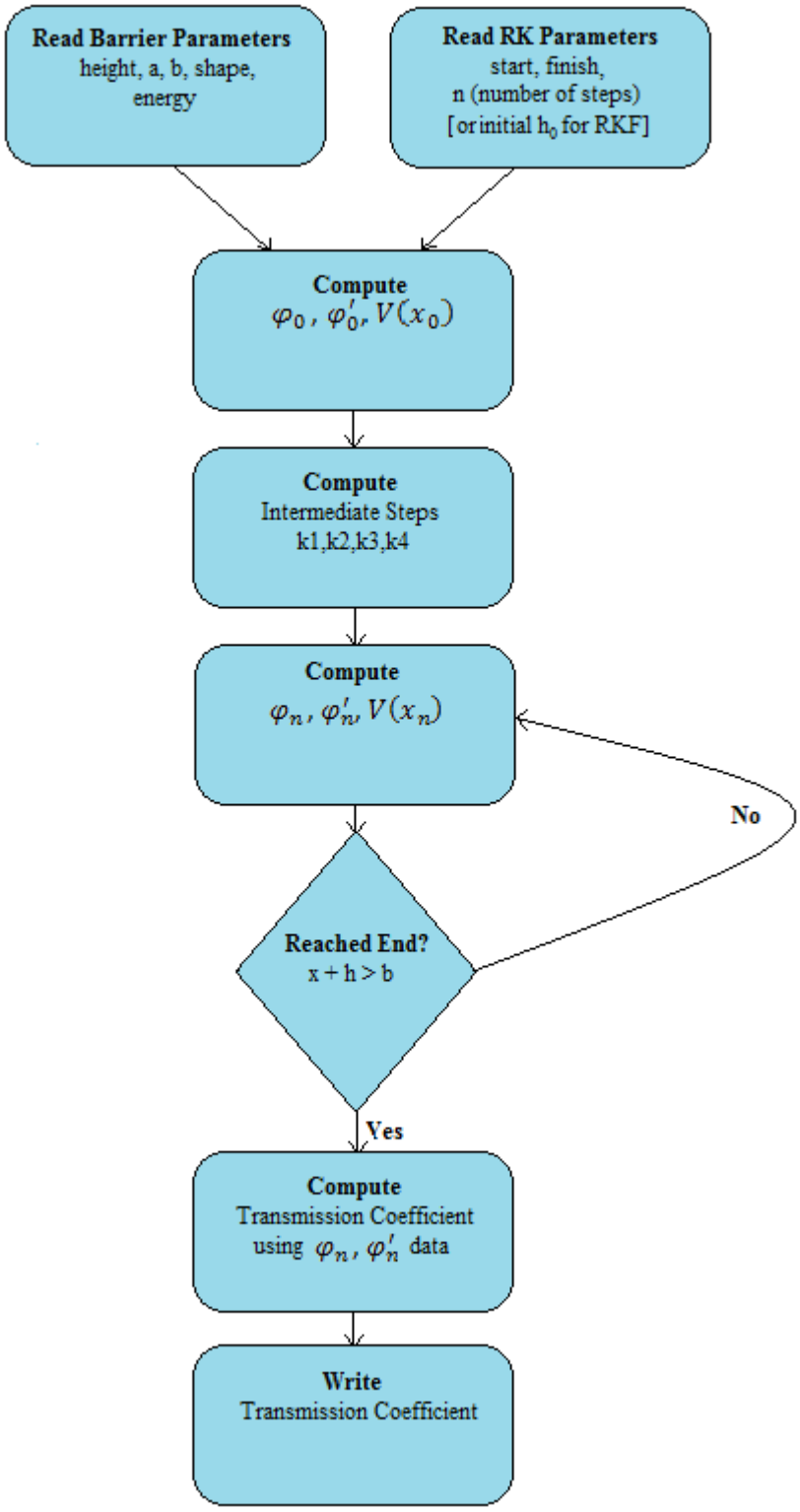

FIGURE 3.6: Flow Chart for the program.

Chapter 4

Testing

4.1 Assessing the Validity of Results

Throughout this project it has been an aim to make sure all results are reliable and easily repeatable. To that effect, there are a number of simple tests that have been included here to verify the various parts of the problem. Firstly, the Runge-Kutta method is verified by solving a simple coupled first order ODE, whose solution can be worked out analytically. To check that potential barriers have been coded in correctly, plots of barrier height against distance x can be produced, and solutions of the Schrödinger equation are then checked by using a rectangular barrier whose results can be worked out by hand.

4.2 Testing the Runge-Kutta Method

In essence the main part of our program that is doing most of the maths is an ODE solver. To test it, all we need to do is replace our TISE with a much simpler second order ODE which we can analytically test the solutions of.

$$\ddot{x}(t) = -x(t) \tag{4.1}$$

This is the ODE for the simple harmonic oscillator (with all constants equal to 1). Notice that this equation is actually very similar to the TISE. By renaming Ψ to x and x to t, and setting $V = 0$, the TISE becomes equation 4.1 (with different constants), making this a particularly relevant test. We can see that a solution of the form $x(t) = cos(t)$ is valid and hence by inputting equation 4.1 into the RK method, we should have data corresponding to the cosine function. By substitution and restructuring the problem as we did in Chapter 3.2.1

$$\mathbf{u'} = \begin{pmatrix} u^{(2)} \\ -u^{(1)} \end{pmatrix} \tag{4.2}$$

Figure 4.1 shows the results of our program after using equation 4.2 and we can easily see that this corresponds well with the cosine function. Hence we can reliably use the Runge-Kutta method.

t	x
6.3	1.0
6.1	1.0
5.9	0.9
5.7	0.8
5.4	0.7
5.2	0.5
5.0	0.3
4.8	0.1
4.6	-0.1
4.4	-0.3
4.2	-0.5
4.0	-0.7
3.8	-0.8
3.6	-0.9
3.4	-1.0
3.1	-1.0
2.9	-1.0
2.7	-0.9
2.5	-0.8
2.3	-0.7
2.1	-0.5
1.9	-0.3
1.7	-0.1
1.5	0.1
1.3	0.3
1.0	0.5
0.8	0.7
0.6	0.8
0.4	0.9
0.2	1.0
0.0	1.0

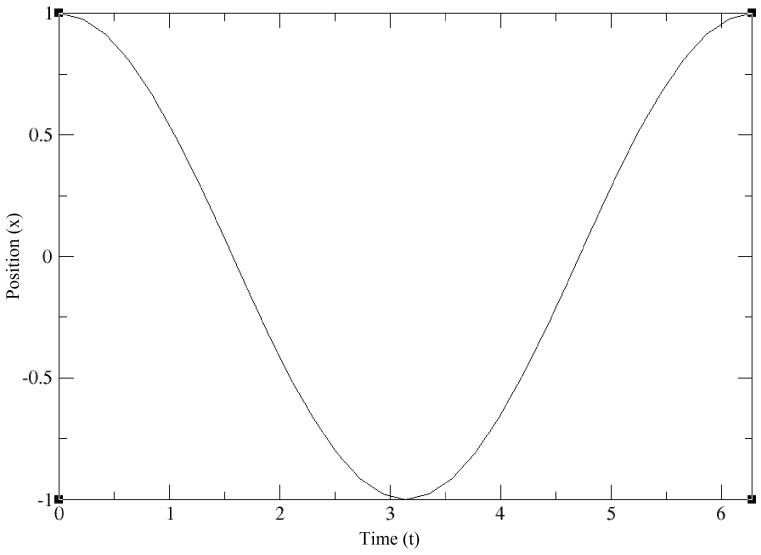

FIGURE 4.1: Results for our simple harmonic oscillator test on the Runge Kutta method.

4.3 Testing the Potential Barrier

The various shapes used as potential barriers have been coded up using a piece wise method. Since they are not usually continuous this means that errors could arise if the function were not defined along the whole real axis. To combat this, plotting the barrier shape should reveal if there are gaps in the definition of each barrier. Figure 3.3 illustrates various barriers that have been plotted.

4.4 Testing the TISE

Since we are sure that the potential barriers are functioning correctly, we can now use the rectangular barrier as a test for the time independent Schrödinger equation. First we can check the initial conditions. As we start on the right hand side with a wavefuntion of only one component, we know that the modulus of the wavefunction squared, after exiting the barrier, should be constant. This can be seen by taking the square of the modulus of equation 3.4 with $B = 0$.

$$|\Psi|^2 = |A\exp(ikx)|^2 \tag{4.3}$$

Since the modulus of the exponent is 1, we can see that $|\Psi|^2 = |A|^2$. So for all calculations using the correct initial conditions, a graph of $|\Psi|^2$ against position, should always show a straight line

after the barrer. Figure 4.2 shows that this is indeed the case. Similarly, we may use 3.4 to show that the results of the program along the whole plane agree with what we have calculated analytically.

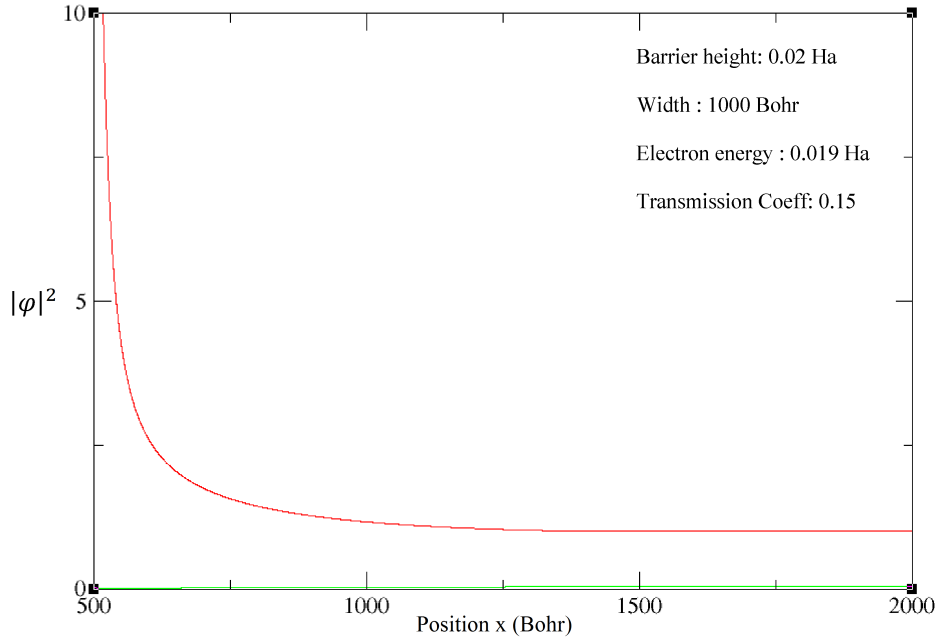

FIGURE 4.2: Checking that the value of $|\Psi^2|$ is constant after the barrier.

We can also test the TISE by examining the transmission coefficient for an electron passing through a square barrier. The shape of the plot has a well documented form which we will be able to compare [9]. Figure 4.3 shows that our results do indeed align with expectations.

4.5 Confidence in Results

With all the boxes ticked, we may now go on to trying barrier shapes of complex forms, such as the Schottky Barrier, that we cannot so easily find the analytical result for. However we know that the results achieved from new tests are reliable and repeatable, regardless of their possible deviation from expectations. It is recommended that should the reader wish to further these studies, either by using the programs provided in the appendix, or other similar programs, that tests are repeated to make sure that all results are consistent. When swapping from one ODE solving algorithm to another, such as we have done with RK and RKF algorithms, it is also useful to compare results frequently as, although they will differ due to the order of each algorithm's truncation error, they should still be very similar and hence will be a good test for each other.

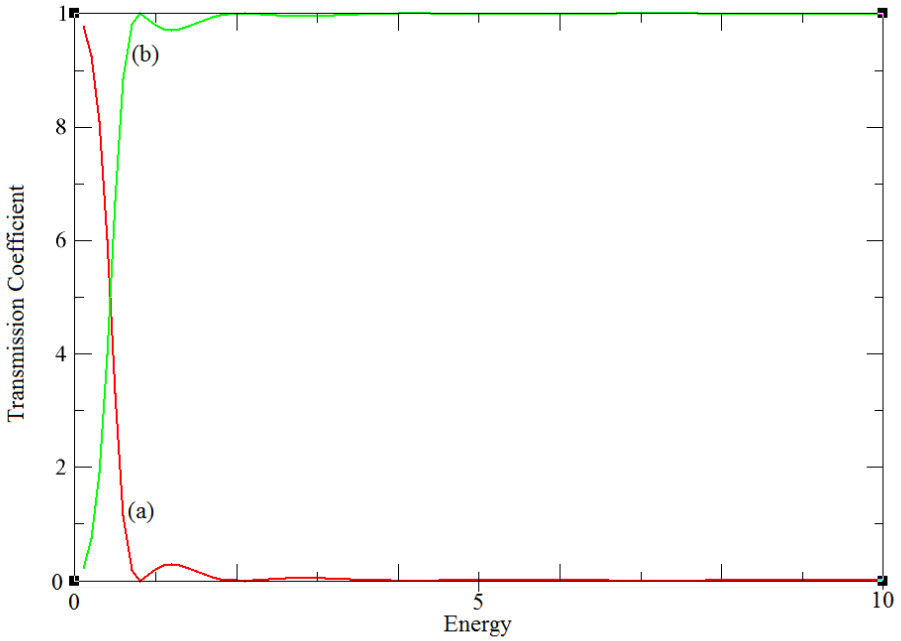

FIGURE 4.3: Graph of electron energy against transmission and reflection coefficient for an electron passing through a square barrier.

Chapter 5

Results

5.1 Typical Schottky Barrier

From Rhoderick and Williams[6] we know that the typical form for a SB is a vertical barrier followed by parabolic decline (as in 2.2). Hence we should first examine the transmission probability as a function of energy. It should be noted that as energy in increased, this will be qualitatively the same as increasing the temperature in the environment of the semiconductor. This is because the average energy of the electrons in the semiconductor is determined by $k_B T$ [9]. Figure 5.1 shows the energy - T coefficient relation for a barrier of height $0.02\ Ha$ and a width of $1000\ a_o$.

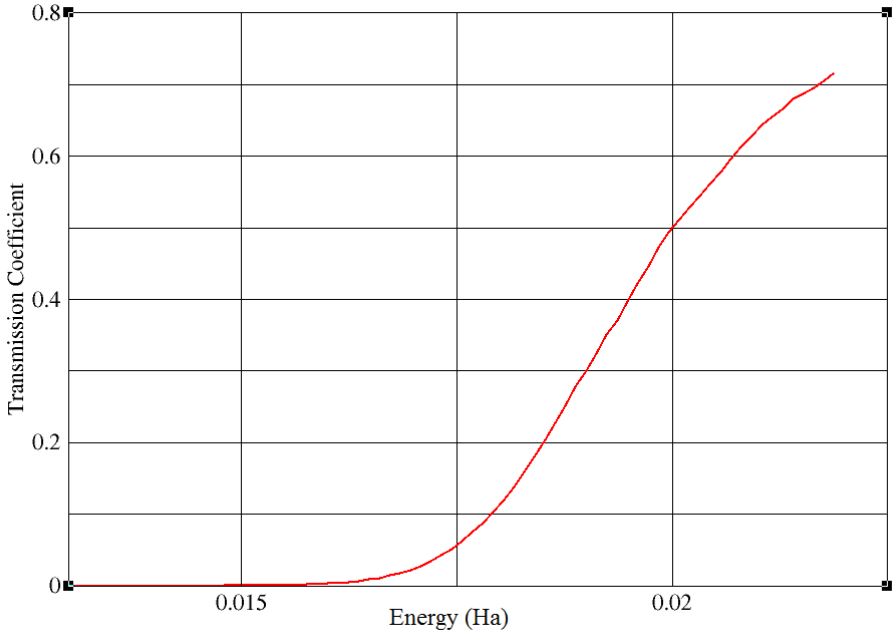

FIGURE 5.1: Graph of energy against transmission coefficient for a barrier of height $0.02\ Ha$ and width $1000\ a_o$.

At an energy $\frac{3}{4}$ the height of the barrier, the transmission probability remains at near zero value, hence tunnelling will only occur at energies close to the top of the barrier. Tunnelling probability

then slowly increases until an energy of about $0.017\ Ha$ which corresponds well with the Field Emission regime. In a heavily doped semiconductor at low temperature, the increase in T arises from the tunnelling of electrons with energies close to the Fermi energy in the semiconductor. As the energy is increased further, the transmission probability also rises rapidly. This is because the electrons 'see' a thinner and lower barrier, corresponding with Thermionic-Field Emission.

A subtle point, that must be noted, is the meaning of the T coefficient. Although it shows us that the probability of an electron tunnelling through the top of the barrier is high, this does not mean that there is necessarily a higher quantity of electrons passing through at that energy. At low temperatures where the average energy of electrons is the fermi energy, there will be a small percentage of electrons with energy at TFE level. These electrons will have a high probability of passing through the barrier, but will only be a small contribution to the current, due to being far from the average energy.

5.1.1 WKB Theory

We can now make a comparison with the transmission probability predicted by Padovani and Stratton[10], which uses the TISE with a WKB (Wentzel–Kramers–Brillouin) approximation and triangular barrier. The equation they came up with is

$$T = exp\left\{-\frac{2}{3}(\Delta E)^{\frac{3}{2}}/E_{00}V_d^{\frac{1}{2}}\right\} \tag{5.1}$$

This means that tunnelling probability should be a function of the difference between barrier height and electron energy, ΔE, the diffusion potential through the barrier, V_d, and a parameter E_{00}. E_{00} is a property of the bulk semiconductor; it is a function of the semiconductor donor concentration and permittivity. Without knowing what kind of plot this equation will produce, we can immediately see that there is a problem with this approximation when $\Delta E = 0$. According to the equation, T will equal 1 at this point, i.e. the probability of transmission of electrons is 100% at the top of the barrier. This will not be the case as, as we have already discussed, in the quantum world there will still be a less that 100% probability of electrons with energy above that of the barrier, from being reflected[9].

Figure 5.1 is a plot of equation 5.1 using parameters for heavily doped gallium arsenide with a barrier height of $0.02\ Ha$, as well as an energy against T coefficient plot from our program, for a barrier of the same height. The width of (a) is dependant on the values of V_d and E_{00} hence we can say that for some values of these parameters, both lines will start to rise at the same point, and will therefore

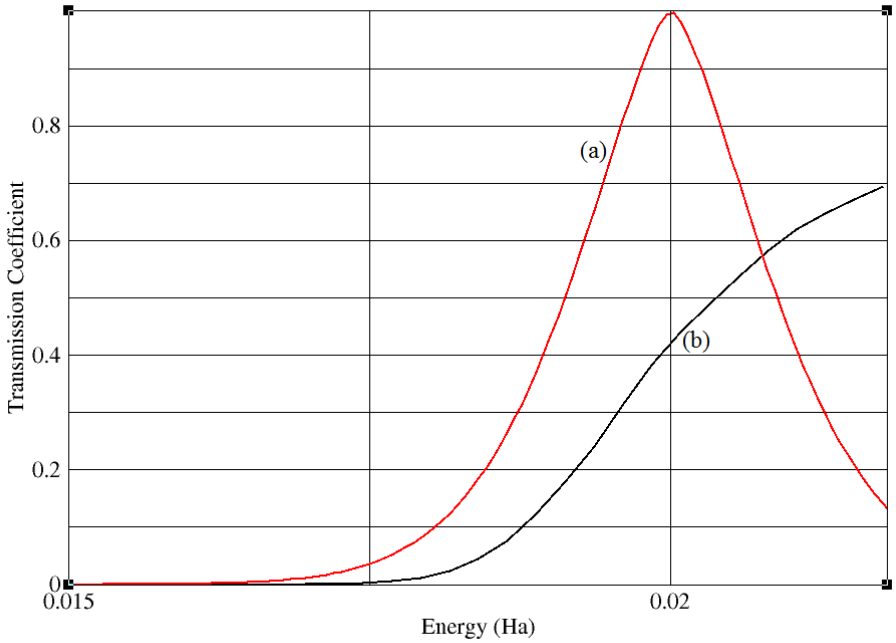

FIGURE 5.2: Plot of transmission coefficient against energy. (a) is the transmission coefficient predicted by Padovani and Stratton while (b) is the data generated by our program.

match up well. However once we go past this initial rise, the probability predicted by Padovani and Stratton starts to rise too quickly and reaches 100% probability, where as our program shows that even at the top of the barrier, the probability is only about 50%.

From this point, the two lines show very different behaviour however we shall not take much from this as Padovani and Stratton's equation is only meant to model electron transmission until the top of the barrier, at which point they believe electron transmission is better modelled by a combination of drift and diffusion theory and thermionic emission. Our plot, (b), shows that the probability will continue to rise as electron energy increases, which intuitively should be the case, since most electrons will not be hampered by the barrier at this point.

5.2 Increasing the Voltage in the SB

The voltage across a Schottky barrier should have a large effect on the ability of electrons to pass through the barrier. A forward bias causes barrier lowering, as well as shortening the depletion region, therefore we expect to see a marked rise in T. Figure 5.3 shows that an

increase in voltage produces a somewhat similar affect as an increase in temperature, or electron energy. Since the Schottky barrier height is lowered as voltage increases, the electrons need to tunnel through less of the barrier and hence the transmission coefficient increases.

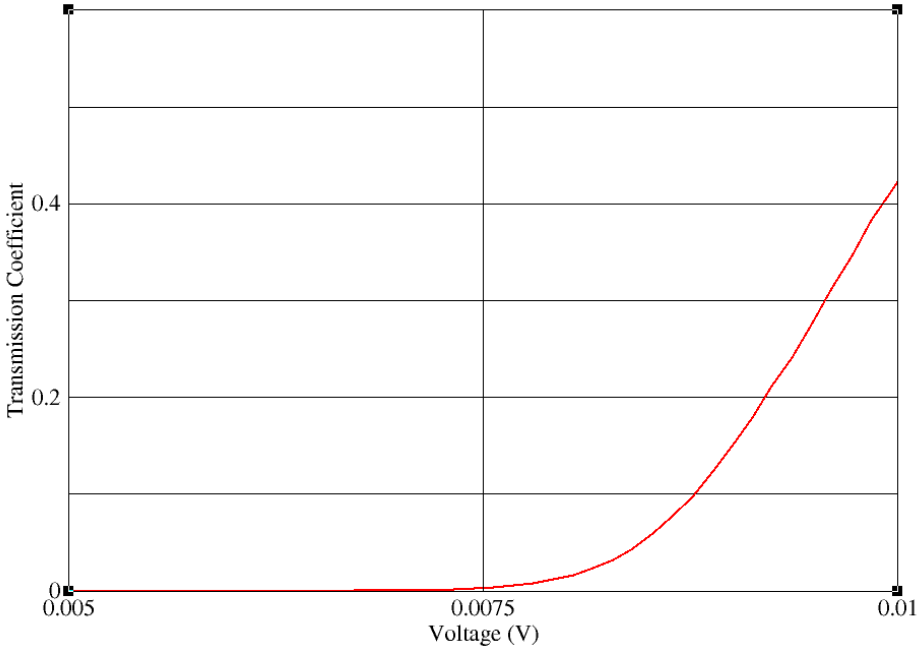

FIGURE 5.3: Graph of voltage against transmission coefficient for a barrier of height $0.02\ Ha$ and width $1000\ a_o$

5.3 Changing the Dimensions of the SB

We now have an idea of what to expect from a Schottky Barrier when it comes to tunnelling through at various energies and how a voltage bias effects the SB, however, we are not sure how this changes as the height or width of the barrier is varied. By collecting data from barriers of various sizes we can form surfaces of constant width or height, which will give an insight into this. Figures 5.4, 5.5 and 5.6 are examples of such barriers. Each figure shows raw data that has not been interpolated and is therefore slightly jagged at certain points. A possible future avenue for this work is to form interpolating polynomials to have more data without the computational cost associated with the calculation of each point.

The constant width surface (figure 5.4) is, in essence, a 3D representation of figure 5.1. We can see that for any height, the transmission coefficient is about 50% when the difference in electron energy is at the top of the barrier, due to the quantum mechanical effects we

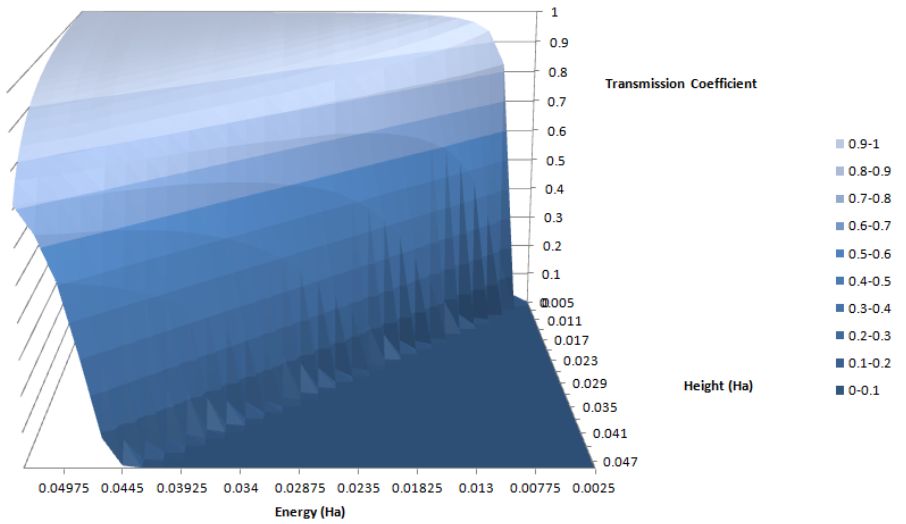

FIGURE 5.4: A constant width surface showing the relationship between electron energy and barrier height. The width for this data is $1000a_o$

have discussed previously. The coefficient then tends to 1 as the energy continues to increase over the barrier height and similarly to 0 as the energy decreases below the barrier height.

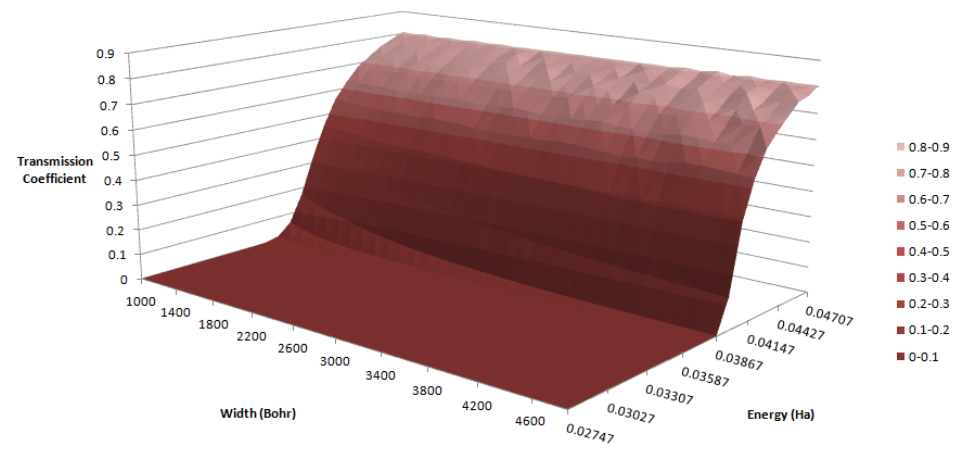

FIGURE 5.5: A constant height surface showing the relationship between electron energy and barrier width. The barrier height for this data is $0.04Ha$

Figure 5.5 is a constant height surface which shows the relationship between electron energy and barrier width. As width increases there is only a subtle decrease in transmission coefficient for the same values of energy. This is somewhat unexpected as we know that the transmission coefficient is dependent on the area of the potential barrier, hence, an increase in width should show a marked decrease in

T. This effect can be explained by the shape of the barrier. In a rectangular barrier, an increase in width will show a large decrease in T since, for any value of energy, the width of potential barrier an electron would have to pass through is the same. However, for our Schottky barrier, after the initial peak in barrier height, the potential starts to decrease according to a parabolic decline. Although the base of the barrier increases by large amounts, near the top of the barrier, where tunnelling becomes noticeable, the barrier width will only have changed by a small percentage. Figure 5.6 shows the same phenomenon, except with respect to height, as opposed to energy. The plot is simply flipped since increases in height lower T, whereas an increase in energy will increase T.

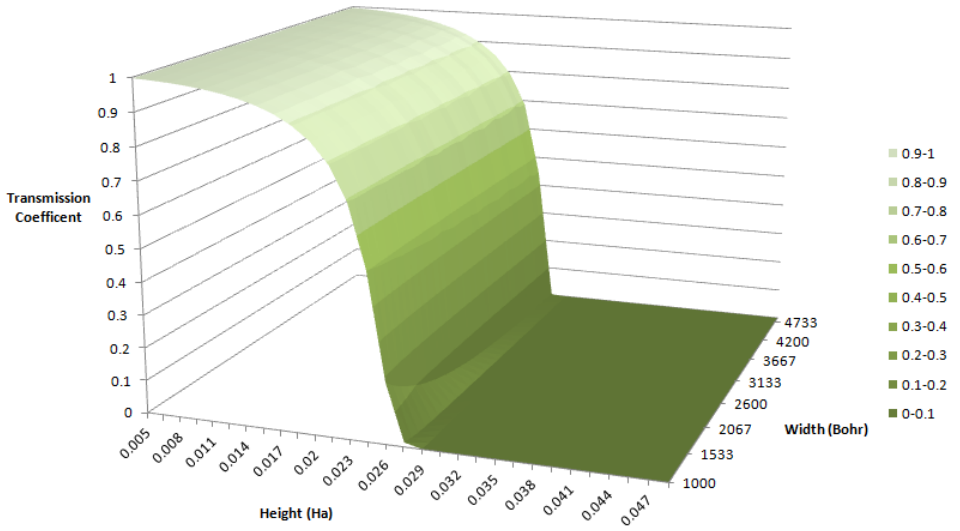

FIGURE 5.6: A constant energy surface showing the relationship between barrier height and width. The electron energy for this data is $0.025\ Ha$

5.4 Applying a Distribution

In the work of Padovani and Stratton[10], the relationship between tunnelling probability and temperature was estimated, as they took the probability found experimentally for electrons tunnelling at a certain temperature, and applied a distribution to the found transmission probability (such as a Gaussian). Since we are able to find the tunnelling probabilities at any energy, we can compare results to see if the old theory aligns well with our results.

We can apply a Gaussian to a distribution of transmission coefficients calculated at various different energies and compare this with data generated from a single coefficient, with a distribution applied

to it to generate more data (as done by P&S). Figure 5.7 shows the plots generated for these two methods.

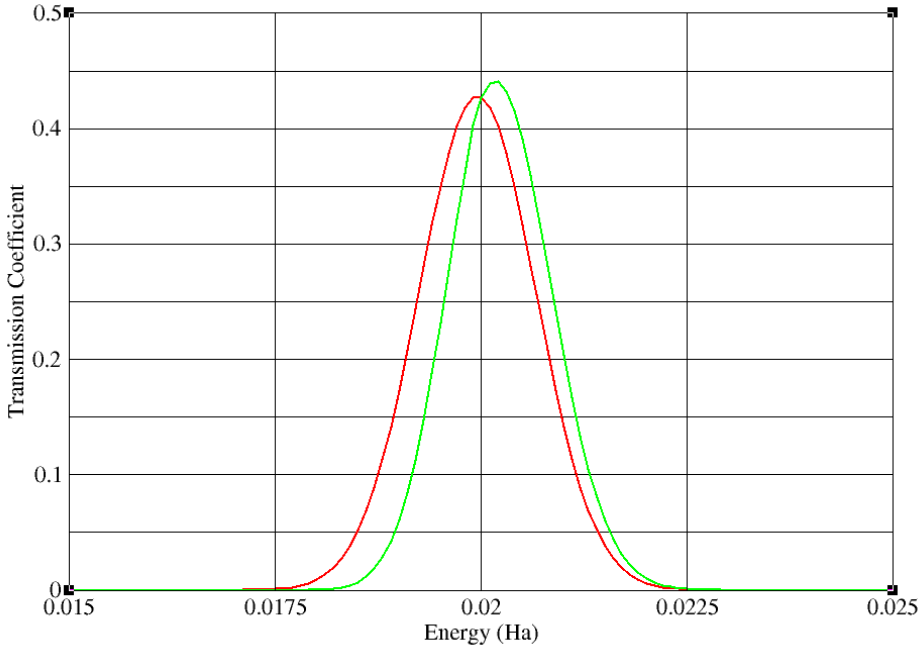

FIGURE 5.7: Gaussian distribution of transmission coefficients, of width k_BT, using Padovani and Strattons method (a) and distributed data from our program (b).

Both plots (a) and (b) look similar, however there are two subtle differences. Plot (a) is a Gaussian distribution of a single transmission coefficient which has created a symmetric function, whereas plot (b) is not strictly a Gaussian as it is made from using a Gaussian distribution on the transmission coefficients we have calculated. These are not constant, as we can see from figure 5.1, and will therefore not form a symmetric function. This is further evidenced by the difference in height between the two plots. The median of both data sets is at energy value $0.02\ Ha$ (the plots intersect here), however, since the transmission coefficient continues to grow as energy increases, the distribution for our plot (b) reaches its apex at a higher energy and at a higher T.

Chapter 6

Conclusion

6.1 General Conclusion

This project set out to examine the quantum mechanical tunnelling properties of an electron passing through a Schottky barrier in a metal-semiconductor junction. To do this we have used a numerical algorithm, the Runge-Kutta method, to solve the 1D time independent Schrödinger equation. From this, we are now able to see how the temperature, or energy of electrons, as well as voltage bias, affect the tunnelling probability of the electron through variably shaped Schottky barriers. In comparison to the work of Padovani and Stratton, we now understand the failings of the old theory due to its poor handling of the quantum mechanical properties of tunnelling through a barrier. We know that these results are repeatable and reliable as they have been thoroughly tested, piece by piece, to make sure that at no point did any component of this study fail to be modelled and understood correctly.

6.1.1 Development of runge_kutta.f90

The program runge_kutta.f90 can model potential barriers of many different forms and can easily be altered to include more functional forms. Its solving algorithm has proven to be very robust so long as the potential and initial conditions are input properly and its performance has been adequate. For extra speed it is recommended to use the Runge-Kutta-Fehlberg algorithm as this has also shown promise albeit with slight modification for handling of discontinuities.

Usage of voltage bias has been coded into the program, however it remains somewhat reliant on a good understanding of how each side of the barrier changes when a forward or backwards bias is applied. It is intended that this functionality will be built upon to allow for easier use.

The input and output of the program can be very easily manipulated by either shell or Perl scripts to produce larger data sets such as those that have been used to produce 2D and 3D graphs e.g. figure 5.1 and 5.4 respectively.

6.2 Further Work

This project has managed to model several of the main parameters in Schottky barriers, however there are still other noticeable phenomena that could be taken into account. Examining the assumptions we have made, such as the absence of an oxide layer over the semiconductor side, or the effect of electrons moving along the interface, rather than simply through it, will help to see the difference between the results we have produced and those found in experiment.

Other important effects we have not studied include image-force lowering, where the electric field over the barrier has the effect of changing the applied bias over it. This causes a reduction in barrier height which will also affect the tunnelling probability to some degree. One could also look to add the theories of drift and diffusion and thermionic emission, models for the transmission of electrons over the barrier, to achieve a more complete understanding of Schottky barriers.

The parameters used in this work are also somewhat difficult to choose in experiment. The height and width of the barrier are more often found to be the result of choosing the semiconductor donor concentration and applied voltage, whereas with this project we skip these and instead choose the dimensions of the barrier artificially. Finding the relation between the barrier shape and the parameters used when engineering SBs could lead to more transferable results, which would be more easily understood and used by experimentalists.

Appendix A

runge_kutta.f90

What follows are several images of the runge_kutta.f90, the program used to solve the TISE for an electron passing through a potential barrier. It is a Fortran code written in modern Fortran 95 or later. The program is made up of 2 modules, rk and ode_schrod.

```
program ode_solver
  use rk
  implicit none

  call read_pot
  call runge_kutta
  call find_coeff

end program ode_solver
```

```
module rk

  use ode_schrod
  implicit none

contains

  subroutine runge_kutta
    !============================================================================!
    ! This is an algorithm for the fourth order Runge Kutta method. It is a 4th !
    ! order ODE solver. However, this method is written so that it starts on    !
    ! b and moves backwards, i.e., opposite to the normal direction             !
    !----------------------------------------------------------------------------!
    ! Input:                                                                     !
    !                                                                            !
    !  a,b : start and end points of the system                                  !
    !  n   : number of iterations (also defines step size through h)             !
    !----------------------------------------------------------------------------!
    ! Requires:                                                                  !
    !  ode_schrod(or test) must be called before running this subroutine         !
    !----------------------------------------------------------------------------!
    ! The input is taken from a file called input1.dat, which must be present    !
    ! when the program is run                                                    !
    !============================================================================!
    implicit none

    !parameters
    integer                         :: i,n,ierr
    real(kind=dp)                   :: x,h,start,finish,wave_n
    complex(kind=dp), dimension(2) :: w,k1,k2,k3,k4

    !read in input parameters
    open(10,file='input1.dat',status='old',iostat=ierr)
    if (ierr/=0) stop "Error in opening input.dat"
    read(10,*) start,finish
    read(10,*) n
    close(unit=10,iostat=ierr)
    if (ierr/=0) stop "Error in closing input.dat"

    !calculate starting psi and psi'
    wave_n = sqrt(2.0_dp*E)
    w(1)   = exp(cmplx(0.0_dp,wave_n,kind=dp)*finish)
    w(2)   = cmplx(0.0_dp,wave_n,kind=dp)*w(1)
    h      = (finish-start)/real(n,dp)
    x      = finish


    !Start writing output data
    open(15,file='output.dat',status='replace',iostat=ierr)
    if (ierr/=0) stop "Error in opening output.dat"
    write(15,*) x,real(w(1)),aimag(w(1)),real(w(2)),aimag(w(2))
    !write(15,"(F5.1,F5.1)") x,real(w(1))

    do i=1,n
       ! 4 function calls, each depends on the preceding one
       k1 = h*f(x,w)
       k2 = h*f(x-(h/2.0_dp),w-(k1/2.0_dp))
       k3 = h*f(x-(h/2.0_dp),w-(k2/2.0_dp))
       k4 = h*f(x-h,w-k3)

       w  = w - (k1+2.0_dp*k2+2.0_dp*k3+k4)/6.0_dp
       x  = x - h
       write(15,*) x,real(w(1)),aimag(w(1)),real(w(2)),aimag(w(2))|

    end do

    close(15,iostat=ierr)
    if (ierr/=0) stop "Error in closing output.dat"

    return
  end subroutine runge_kutta

end module rk
```

```
module ode_schrod
  implicit none

  integer, parameter             :: dp=selected_real_kind(15,300)

  !constants
  real(kind=dp), parameter :: pi        = 3.14159265358979323846264338327950288_dp

  !dimensions and shape of the potential
  character(len=20), save        :: pot_form
  real(kind=dp), save            :: a,b,c,d,height,E,Vol

  !calculated constants
  real(kind=dp), save            :: para_cons

contains

  subroutine read_pot
    !=========================================================================!
    ! Reads the form and dimentions of the given potential from a file,       !
    ! input2.dat (This will already have been opened previously in a           !
    ! different subroutine)                                                   !
    !-------------------------------------------------------------------------!
    ! This subroutine need to be called before using the Runge Kutta          !
    ! method, if the ode is going to be the shrodinger equation               !
    !=========================================================================!
    implicit none

    integer :: ierr

    open(10,file='input2.dat',status='old',iostat=ierr)
    if (ierr/=0) stop "Error in opening input.dat"
    read(10,*) pot_form
    if (pot_form=='triangle') then
       read(10,*) height,a,b
    else if (pot_form=='parabolic_triangle') then
       read(10,*) height,a,b
    else if (pot_form=='rectangle') then
       read(10,*) height,a,b
    else if (pot_form=='double_rectangle') then
       read(10,*) height,a,b,c,d
    else if (pot_form=='trapezoid') then
       read(10,*) height,a,b,c,d
    else
       stop "Invalid potential name"
    end if

    read(10,*) E
    read(10,*) Vol

    !calculate some constants for later
    para_cons  = (height-Vol)/(a**2 - 2.0_dp*b*a + b**2)

    close(10,iostat=ierr)
    if(ierr/=0) stop "Error in closing input.dat"

    return
  end subroutine read_pot
```

```
function f(x,w)
  !=====================================================================!
  ! Defines the ode under study. This is the Schrödinger Eqn            !
  !---------------------------------------------------------------------!
  ! Requires function V(x)                                              !
  !---------------------------------------------------------------------!
  ! Units:                                                              !
  ! The TISE has been written using atomic units, therefore             !
  ! x is in Hartrees                                                    !
  ! E is in Bohrs                                                       !
  !=====================================================================!
  implicit none
  real(kind=dp), intent(in)                  :: x
  complex(kind=dp), dimension(2), intent(in) :: w
  complex(kind=dp), dimension(2)             :: f

  f(1) = w(2)
  f(2) = 2*(V(x)-E)*w(1)

  return
end function f

real(kind=dp) function V(x)
  !=====================================================================!
  !| This function take the constants read in by read_pot and then      !
  ! calculates a value for the potential at a particular value of x     !
  !---------------------------------------------------------------------!
  ! Requires:                                                           !
  ! read_pot                                                            !
  !---------------------------------------------------------------------!
  ! x is in units of Bohr (atomic units)                                !
  !=====================================================================!
  implicit none
  real(kind=dp), intent(in) :: x

  if (pot_form=='triangle') then
     if (x .lt. a) then
        V=0.0_dp
     else if (x .ge. a .and. x .le. b) then
        V=((Vol-height)*x)/(b-a) + height - ((Vol-height)*a)/(b-a)
     else if (x .gt. b) then
        V=Vol
     end if

  else if (pot_form=='parabolic_triangle') then
     if (x .lt. a) then
        V=0.0_dp
     else if (x .ge. a .and. x .le. b) then
        V= para_cons*x**2 - 2.0_dp*para_cons*b*x + Vol + para_cons*b**2
     else if (x .gt. b) then
        V=Vol
     end if

  else if (pot_form=='rectangle') then
     if (x .lt. a) then
        V=0.0_dp
     else if (x .ge. a .and. x .le. b) then
        V=(Vol*x)/(b-a) + height - (Vol*a)/(b-a)
     else if (x .gt. b) then
        V=Vol
     end if
```

```
   else if (pot_form=='rectangle') then
      if (x .lt. a) then
         V=0.0_dp
      else if (x .ge. a .and. x .le. b) then
         V=(Vol*x)/(b-a) + height - (Vol*a)/(b-a)
      else if (x .gt. b) then
         V=Vol
      end if

   else if (pot_form=='double_rectangle') then
      ! Currently this potential is not coded for non-zero Voltages
      if (Vol .le. -0.0001_dp .or. Vol .ge. 0.0001_dp) then
         stop "Error: potential not coded to use non-zero Voltage"
      end if

      if (x .lt. a) then
         V=0.0_dp
      else if (x .ge. a .and. x .le. b) then
         V=height
      else if (x .gt. b .and. x .lt. c) then
         V=0.0_dp
      else if (x .ge. c .and. x .le. d) then
         V=height
      else if (x .gt. d) then
         V=0.0_dp
      end if

   else if (pot_form=='trapezoid') then
      ! Currently this potential is not coded for non-zero Voltages
      if (Vol .le. -0.0001_dp .or. Vol .ge. 0.0001_dp) then
         stop "Error: potential not coded to use non-zero Voltage"
      end if

      if (x .lt. a) then
         V=0.0_dp
      else if (x .ge. a .and. x .le. b) then
         V= height*(x-a)/(b-a)
      else if (x .gt. b .and. x .lt. c) then
         V= height
      else if (x .ge. c .and. x .le. d) then
         V= height + height*(x-c)/(c-d)
      else if (x .gt. d) then
         V=0.0_dp
      end if
   else
      stop "Error finding potential for the input shape"
   end if

   return
end function V
```

```
subroutine find_coeff
  !=============================================================================!
  ! This subroutine goes through the newly created output.dat file and gets     !
  ! the values of psi at x=0 and x=pi/2*k. Then, the values are used to         !
  ! calculate the Reflection coefficient (and hence Transmission)               !
  !-----------------------------------------------------------------------------!
  ! Subroutine must occur after the runge_kutta subroutine.                     !
  ! This is becuase it required the file output.dat to exist                    !
  !-----------------------------------------------------------------------------!
  !                                                                             !
  ! Input:                                                                      !
  !  E : Energy (Hartrees)                                                      !
  !=============================================================================!
  implicit none

  complex(kind=dp) :: psi_1,psi_2,At,Ar
  real(kind=dp)    :: x,Re,Im,k,refl
  integer          :: ierr

  open(15,file='output.dat',status='old',iostat=ierr)
  if (ierr/=0) stop "Error in opening output.dat"

  !find psi at x = 0
  read(15,*) x,Re,Im
  loop1 : do
     if (abs(x) .gt. 1.0e-6_dp) then
        read(15,*) x,Re,Im
     else
        exit loop1
     end if
  end do loop1

  !store value
  psi_1 = cmplx(Re,Im,kind=dp)
  !!print *, x,psi_1

  close(15,iostat=ierr)
  if (ierr/=0) stop "Error in close output.dat"
  open(15,file='output.dat',status='old',iostat=ierr)
  if (ierr/=0) stop "Error in opening output.dat"
```

Appendix B

Shell Script

What follows is a shell script which can be used to generate data for constant width surfaces of electron energy against height. It is intended to give the user an idea of how to incorporate the runge_kutta.f90 program into an automated procedure.

```
#-------------------------------------------------------------------------------------#
# This shell script performs several runs of runge_kutta.dat for various values      #
# of electron energy, barrier width and barrier height. This data is then collected  #
# in a .csv file which can be used to represent the data graphically                  #
#-------------------------------------------------------------------------------------#

#Width in Bohr
width_min=1000
width_max=5000
width_stp=1 #1
width_stp_size=$(awk "BEGIN{print ($width_max - $width_min)/$width_stp}")

#Height in Hartrees
height_min=0.005
height_max=0.05
height_stp=30
height_stp_size=$(awk "BEGIN{print ($height_max - $height_min)/$height_stp}")

#Electron energy in Hartrees
energy_min=$(awk "BEGIN{print 0.5*$height_min}")
energy_max=$(awk "BEGIN{print 0.1*$height_max + $height_max}")
energy_stp=30
energy_stp_size=$(awk "BEGIN{print ($energy_max - $energy_min)/$energy_stp}")

# Arrays contaigning data to be written to file
energy_array1=()
energy_array2=()

for (( i=1; i<=$width_stp; i++ ))
do
    width=$(awk "BEGIN{print $width_min + ($i-1)*$width_stp_size}")
    width_start=$(awk "BEGIN{print $width - 0.5*$width}")
    width_end=$(awk "BEGIN{print $width + 0.5*$width}")
    boundary=$(awk "BEGIN{print 2*$width_end}")

    sed -r -i "s/([0-9]+.*[0-9]*\s+)([0-9]+.*[0-9]*\s+)([0-9]+.*[0-9]*\s+)(::\s+height)/\1 $width_start $width_end \4/" input2.dat
    sed -r -i "s/([0-9]+.*[0-9]*\s+)([0-9]+.*[0-9]*\s+)(::\s+start\s+finish)/0.0 $boundary \3/" input1.dat

    for (( x=1; x<=$energy_stp; x++ ))
    do
        energy=$(awk "BEGIN{print $energy_min + ($x-1)*$energy_stp_size}")
        energy_array1+=("$energy ,")
    done

    echo "$width ${energy_array1[*]}"  >> EvH_data_${width}.csv
    energy_array1=()

    for (( j=1; j<=$height_stp; j++ ))
    do
        height=$(awk "BEGIN{print $height_min + ($j-1)*$height_stp_size}")

        sed -r -i "s/([0-9]+.[0-9]*\s+)([0-9]+.[0-9]*\s+)([0-9]+.[0-9]*\s+)(::\s+height)/$height \2\3\4/" input2.dat

        for (( k=1; k<=$energy_stp; k++ ))
        do
            energy=$(awk "BEGIN{print $energy_min + ($k-1)*$energy_stp_size}")

            sed -r -i "s/([0-9]+.*[0-9]*\s+)(::\s+energy)/$energy \2/" input2.dat

            temp=$(./solution.exe)
            energy_array2+=("$temp ,")

        done

        echo "$height ,${energy_array2[*]}" >> EvH_data_${width}.csv
        energy_array2=()

    done
done
```

Bibliography

[1] A. J. Vick. *Measuring Low Dimensional Schottky Barriers of Rare Earth Silicide-Silcon Interfaces*. 2011.

[2] V. V. Osipov and A. M. Bratkovsky. "A class of spin injection-precession ultrafast nanodevices". In: *Applied Physics Letters* 84.12 (2004).

[3] A. M. Bratkovsky. "Spintronic effects in metallic, semiconductor, metal–oxide and metal–semiconductor heterostructures". In: *Reports on Progress in Physics* 71.2 (Jan. 2008).

[4] K. Lee T. Bland and S. Steinmüller. "The spintronics challenge". In: *Physics World* 21.1 (2008).

[5] D. D. Awschalom and M. E. Flatté. "Challenges for semiconductor spintronics". In: *Nature Physics* 3.3 (2007).

[6] E. H. Rhoderick and R. H. Williams. *Metal-semiconductor contacts*. 2nd ed. Clarendon Press, 1988.

[7] R. L. Burden and J. D. Faires. *Numerical Analysis*. Brooks,Cole, 2001.

[8] J. M. Thijssen. *Computational Physics*. 2nd ed. Cambridge University Press, 2007.

[9] A. I. M. Rae. *Quantum Mechanics*. 5th ed. Taylor and Francis, 2007.

[10] F. A. Padovani and R. Stratton. "Field and thermionic-field emission in Schottky barriers". In: *Solid-State Electronics* 9.7 (1966).